

Electronic Supplementary Information

Mixed polyvinyl pyrrolidone hydrogel-mediated synthesis of high-quality Ag nanowires for high-performance transparent conductors

Mei Han,^a Yongjie Ge,^a Jianfang Liu,^a Zhongzhong Cao,^a Moxia Li,^a Xidong Duan,^{*a} Jiawen Hu,^{*a}

[†]Hunan Key Laboratory of Two-Dimensional Materials, State Key Laboratory for Chemo/Biosensing and Chemometrics, College of Chemistry and Chemical Engineering, Hunan University, Changsha 410082, China

*To whom correspondence should be sent. Prof. X. Duan: xidongduan@hnu.edu.cn and Prof. J. Hu: jwhu@hnu.edu.cn.

1. Experimental section

Chemicals and Materials. N-vinyl-2-pyrrolidone (NVP, AR) and 0.125 mm-thick polyethylene glycol terephthalate (PET) film were purchased from Aladdin Chemistry Co., Ltd (Shanghai, China) and Shanghai Feixia Rubber and Hardware Co., Ltd (Shanghai, China), respectively. Silver nitrate (AR), polyvinyl pyrrolidone (PVP, K30), copper chloride (AR), melamine (99%), acetone (AR), NaBH₄ (98%), ethylene glycol (EG, AR), and ethanol (AR) were purchased from Sinopharm Chemical Reagent Co., Ltd (Shanghai, China). All the chemicals were used as received without further purification. Ultrapure water (≥ 18.2 M Ω -cm) purified from an RS2200QSS-PURIST ultrapure water system (Rephile Bioscience, Ltd. Shanghai, China) was used throughout all the experiments.

Preparation of the mixed PVP hydrogel. Mixed PVP (m-PVP) hydrogel was prepared by the crosslinking of NVP monomers (i.e., the precursor of commercial PVP) using g-C₃N₄ as the initiator. Briefly, C₃N₄ powders were synthesized by one-step polymerization of melamine at 550 °C in a muffle furnace.¹ The resultant yellow C₃N₄ powders were collected and dispersed in ultrapure water, followed by vigorous sonication for 48 h. During sonication, g-C₃N₄ nanosheets (average diameter, ~20 nm) were exfoliated from the C₃N₄ powders, forming a nearly transparent solution. After centrifugation at 10000 rpm for 10 min, the supernatant was collected and stored as a g-C₃N₄ nanosheet solution. The resultant m-PVP hydrogel was formed by mixing g-C₃N₄ nanosheet solution (2 mL) and NVP (8 mL) in a 20 mL vial while magnetic stirring, followed by ultraviolet illumination from a 360 nm LED (12 W) at room temperature for 4 h.

Fabrication of Ag NWs and Ag NW film. Ag NWs were synthesized following the well-established polyol reduction method^{2,3}, but using m-PVP hydrogel instead of commercial PVP as the ligands. Briefly, a certain amount of m-PVP hydrogel was added to EG (20 mL) at room temperature while magnetic stirring, and then the temperature of the mixture was ramped to 160 °C in an oil bath and kept at this temperature for 1 h. To produce AgCl as heterogeneous nucleation sites and form five-fold twinned nuclei (FTN) of Ag, CuCl₂ in EG (35 μ L, 0.01 M) and AgNO₃ in EG (70 μ L, 0.01 M) were sequentially added at a time interval of 30 min. Then, AgNO₃ in EG (7 mL, 0.1 M) was added at a rate of 0.5 mL/min. Upon the addition of AgNO₃, the reaction was continued at 160 °C for about 30 min and then the mixture was naturally cooled down to room temperature. The resultant m-PVP-wrapped Ag NWs were collected by centrifugation (2000 rpm, 10 min) and redispersed in ethanol, forming a stock ethanolic dispersion (1.0 mg/mL). For comparison, PVP-wrapped Ag NWs were synthesized according to the polyol-reduction methods. The resultant PVP-wrapped Ag NWs were separated from the dispersion by the addition of acetone, further cleaned by 3 cycles of centrifugation (2000 rpm, 10 min) and redispersion in ethanol, and finally stored in ethanol (0.8 mg/mL). The yield of the m-PVP-wrapped Ag NWs is calculated according to the following formula

$$\eta = \frac{w_a}{w_t}$$

Here, η , w_a , and w_t represent the yield of the Ag NWs synthesized, their actual weight (weighed after removal of excess ligand and Ag NPs), and their theoretical weight (calculated by assuming that all the Ag nutrition from AgNO₃ are exploited for the growth of Ag NWs).

Prior to the fabrication of Ag NW thin films, the PET substrate was sequentially cleaned by sonication in alcohol and ultrapure water. To improve its hydrophilicity, the PET substrate was further cleaned in oxygen plasma (SmartPlasma, PlasmaTechnology GmbH, Germany) at 70 W for 5 min. Ag NW film was fabricated by spin coating the Ag NW dispersion (100 μ L, 1.0 mg/mL) on a cleaned PET substrate (20 mm \times 20 mm). The sheet resistance and transmittance of the Ag NW thin film can be tuned by controlling the NW areal density. For comparison, surface-cleaned Ag NW film was obtained by immersing the m-PVP-wrapped Ag NW film in 0.5 M NaBH₄ solution for 30 s, which results in complete removal of the m-PVP ligands.⁴

Construction of single Ag NW device. The in-place carrier transport properties of the Ag NW film are mainly dictated by the contact resistance at the NW/NW junction. To measure the contact resistance at the NW/NW junction, single Ag NW devices without and with a NW/NW junction were constructed. Briefly, Ag electrode pairs (thickness, 60 nm) with a channel of 30 μ m were defined through a mask on a clean glass substrate by thermal evaporation. Then, single Ag NW devices with or without a NW/NW junction were deposited in the channel by spin coating dilute dispersion of Ag NW in ethanol (100 μ L, 0.001 mg/mL), followed by drying in the air.

Construction of electron-only device. To evaluate the out-of-plane carrier transport properties of the Ag NW film, stacked electron-only devices were constructed following our previous work⁴. Briefly, Ag NW films were fabricated by spin coating in a rectangular area (5 mm \times 15 mm) defined on a clean PET substrate using a 3M tape. Then, a semiconductor layer of fullerene (C₆₀, 150 nm) and Ag electrode (top electrode, 60 nm thickness) were sequentially evaporated through a mask (area, 0.04 cm²) using a JSD-300 vacuum evaporator (Anhui Jiashuo Vacuum Science and Technology Co., Ltd, China).

Characterizations. Gel-permeation chromatography (GPC) was carried out on a Waters Breeze 2 GPC system equipped with two PLgel columns (5 μ m MIXED-C, 30 \times 7.5 mm) and a RI detector. HPLC-grade DMF with 0.1% LiBr was used as the mobile phase, and samples were run at a flow rate of 1 mL \cdot min⁻¹ and 60 $^{\circ}$ C. The GPC was calibrated using polystyrene (PS) standards (EasiVial PS-M 2 mL) or PEG standards kit (EasiVial PEG/PEO 2 mL) from Agilent Technologies. Fourier-transform infrared (FT-IR) spectra were measured on an IRTracer-100 spectrometer (Shimadzu, Japan) using KBr pellet. Raman spectra were measured on an inVia Reflex micro-Raman spectrometer (Renishaw, U.K.) using 632.8 nm He-Ne laser as the excitation source. Carbon nuclear magnetic resonance spectroscopy (¹³C NMR) measurements were performed on a Bruker AV400 MHz NMR spectrometer. All NMR spectra were measured relative to the signals for residual chloroform (77.00 ppm for ¹³C) in the deuterated solvent and were reported in ppm relative to trimethylsilane ($\delta = 0$). Scanning electron microscopy (SEM) images were obtained on an Σ IGMA SEM microscope (Zeiss, Germany). High-resolution transmission electron microscopy (HRTEM) images and selected-area electron diffraction (SAED) patterns were obtained on a Titan G2 60-300 transmission electron microscope (FEI, USA). Powder X-ray diffractions (XRD) were performed on an XRD-6100 X-ray diffractometer (Shimadzu, Japan) using CuK ($\lambda = 0.154$ nm) radiation as an incident beam. Dark-field optical images of the Ag NWs and Ag NPs were obtained on a BX51 fluorescence microscope (OLYMPUS, Japan) mounted with a DP27 digital color camera (OLYMPUS, Japan). Total transmittance (T_{total}) and diffuse transmittance (T_{diffuse}) spectra of the Ag NW films were obtained on a UV-3600 spectrometer with an integrating sphere (Shimadzu, Japan) using a PET substrate as reference. T_{total} is the sum of direct transmittance (T_{direct}) and T_{diffuse} , *i.e.*, $T_{\text{total}} = T_{\text{direct}} + T_{\text{diffuse}}$. Therefore, the term of Haze, $T_{\text{diffuse}}/T_{\text{total}}$, presents the ratio of light that is transmitted in a diffuse manner and the total light transmitted. The sheet resistance of the Ag NW film was

measured on an RTS-9 four-probe instrument (Guangzhou Four-probe Scientific Co., Ltd, China). Current-voltage (I - V) responses of single Ag NW device and the electron-only devices were measured on a B1500A semiconductor device analyzer (Keysight, America).

2. Supplementary figures and tables

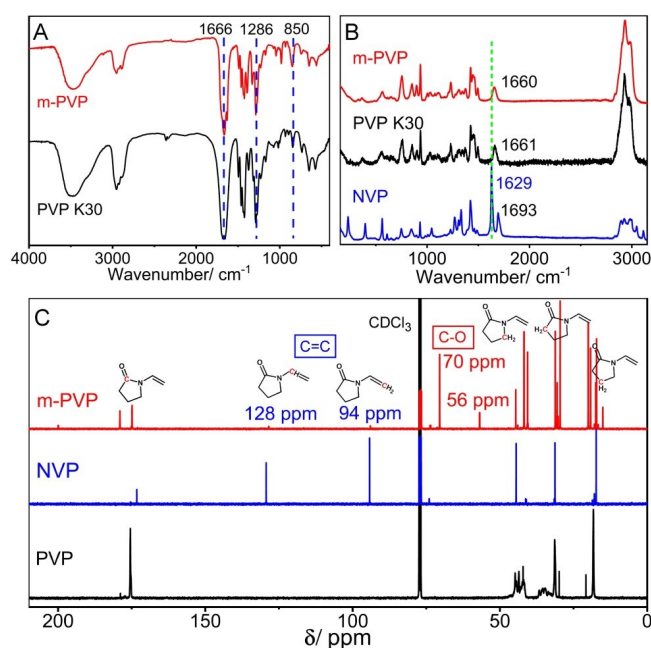


Figure S1. (A) FT-IR spectra of NVP, PVP, and m-PVP xerogel, (B) Raman spectra of NVP, PVP, and m-PVP hydrogel, and (C) ¹³C NMR spectra of NVP, PVP, and m-PVP hydrogel.

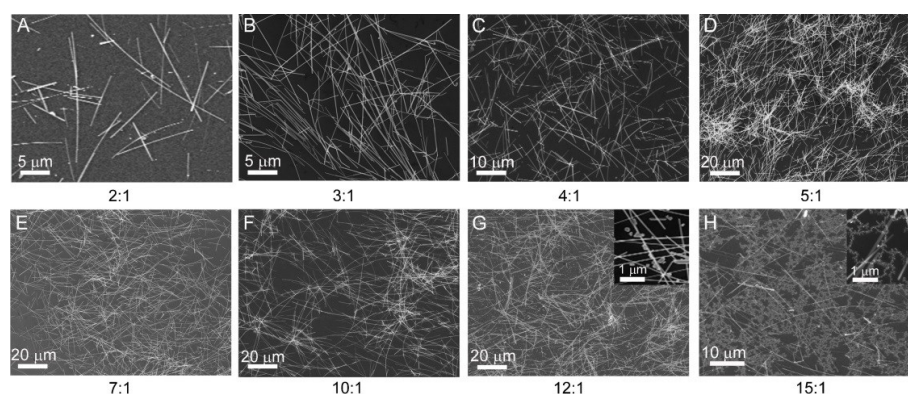


Figure S2. SEM images of Ag NWs synthesized at different molar ratios of m-PVP hydrogel (in term of the amount of the NVP monomer) and AgNO₃: (A) 2 : 1, (B) 3 : 1, (C) 4 : 1, (D) 5 : 1, (E) 7 : 1, (F) 10 : 1, (G) 12 : 1, and (H) 15 : 1. Insets in G and H: high-magnification SEM images of Ag NWs.

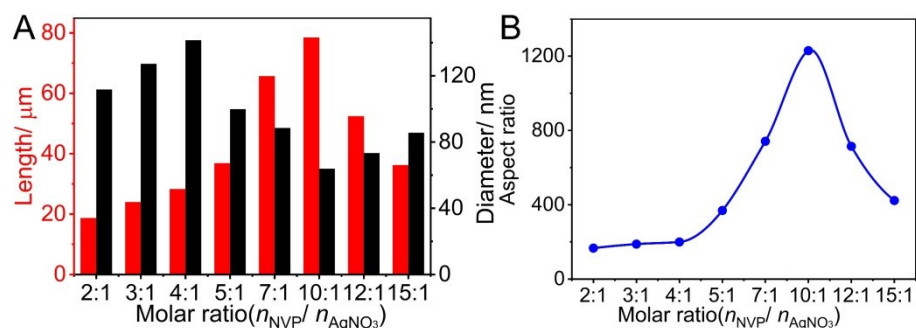


Figure S3. Change of (A) the average diameter and length and (B) aspect ratio for the Ag NWs synthesized at different molar ratios of m-PVP hydrogel (in terms of the amount of NVP monomer) and AgNO₃.

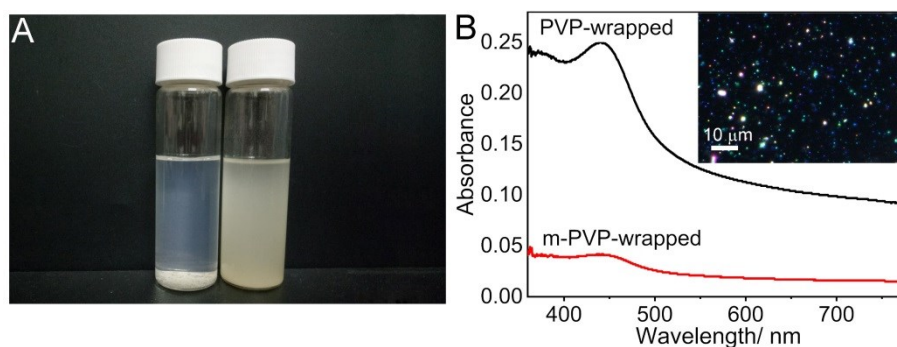


Figure S4. (A) Optical image for m-PVP-wrapped Ag NW dispersion (left, 5 mL) and PVP-wrapped Ag NW dispersion (right, 5 mL) upon addition of acetone (25 mL) for 60 min and (B) UV-Vis spectra for the Ag NPs in their supernatant (collected upon separation of the Ag NPs from the supernatant using high-speed centrifugation and redispersion of the collected Ag NPs in water). Inset in panel B: the dark-field optical image of the Ag NPs in the supernatant of the PVP-wrapped Ag NWs dispersion shown in panel A.

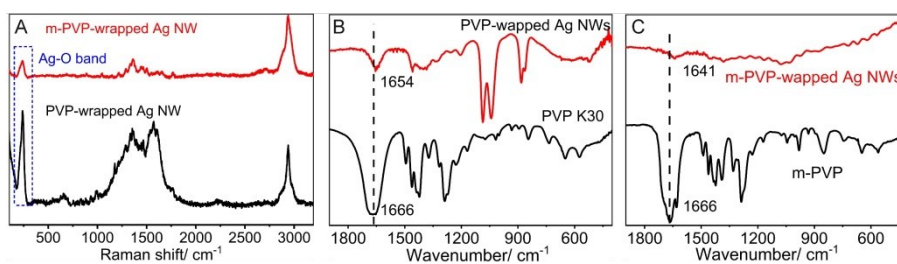


Figure S5. (A) Raman spectra of PVP-wrapped and m-PVP-wrapped Ag NWs, (B) FT-IR spectra of PVP and PVP-wrapped Ag NWs, and (C) FT-IR spectra of m-PVP xerogel and m-PVP-wrapped Ag NWs.

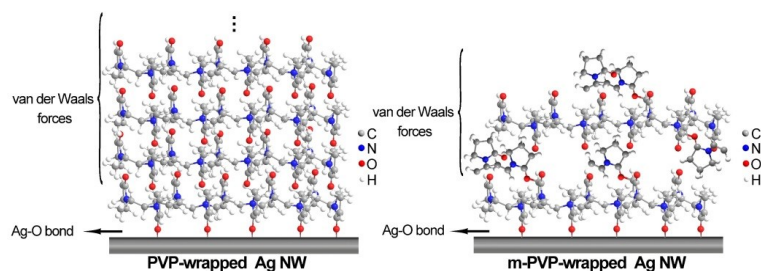


Figure S6. Surface adsorption configuration for PVP and m-PVP on Ag NW.

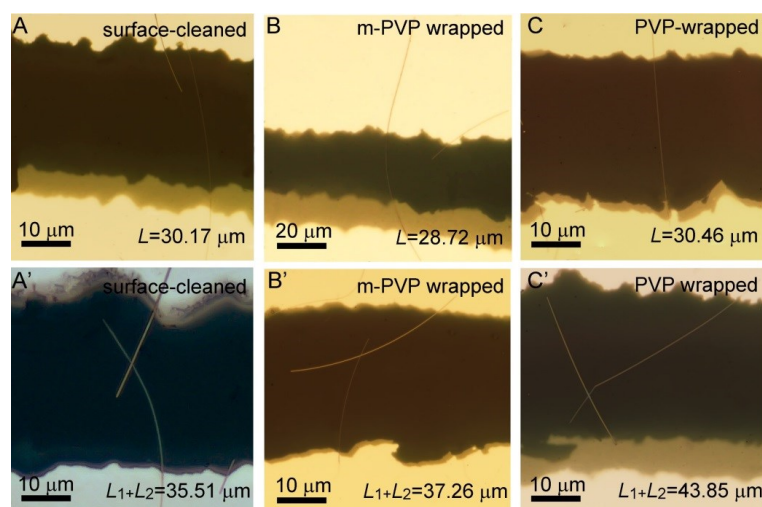


Figure S7. Optical images of single Ag NW devices constructed from (A, A') PVP-wrapped, (B, B') m-PVP-wrapped, and (C, C') surface-cleaned Ag NWs without (A, B, and C) and with (A', B', and C') an NW/NW junction.

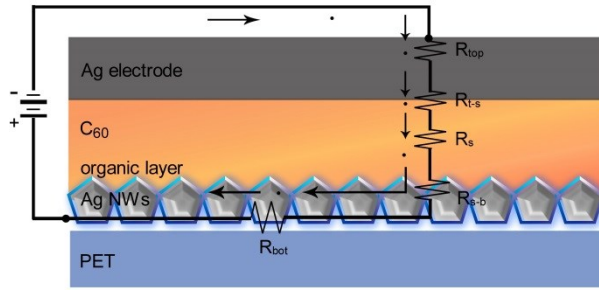


Figure S8. Equivalent electric circuit for the electron-only device constructed from thin Ag NW film using C₆₀ as the semiconductor layer.

Table S1. Overall resistances and resistance components for single Ag NW device constructed surface-cleaned, m-PVP-wrapped, and PVP-wrapped Ag NWs without and with an NW/NW junction.

Single Ag NW device	without a NW/NW junction				with a NW/NW junction		
	R_1 / Ω	R_{NW1} / Ω	$R_{NW/ET} / \Omega$	R_2 / Ω	$R_{NW2,1} + R_{NW2,2} / \Omega$	$2R_{NW/ET} / \Omega$	$R_{NW/NW} / \Omega$
Surface-cleaned	207.6	183.7	11.95	259.0	216.3	23.9	18.8
m-PVP-wrapped	228.5	174.9	26.79	314.2	226.9	53.6	33.7
PVP-wrapped	353.1	135.9	108.60	521.6	195.6	217.2	108.8

R_1 and R_2 are the overall resistance of single Ag NW devices without and with a NW/NW junction, i.e., $R_1 = R_{NW1} + 2R_{NW/ET}$ and $R_2 = R_{NW2,1} + R_{NW2,2} + R_{NW/NW} + 2R_{NW/ET}$, respectively, which can be calculated from the I - V curves of the device. R_{NW} is the resistance of a single Ag NW in the electric circuit and can be calculated by knowing its cross-section area (A , calculated from the average diameter which is 65, 65, and 75 nm for surface-cleaned, m-PVP-wrapped, and PVP wrapped Ag NWs, respectively), length ($L_1=30.17$, 28.72, and 30.46 μm ; $L_{1,2} + L_{2,1} = 35.51$, 37.26, and 43.85 μm , measured from Figure S7), and corresponding resistivity ρ (i.e., $R_{NW} = \rho L/A$). For thin Ag nanowires, their ρ is dependent on the diameter so that their values were taken from the literature⁵, which are 2.02×10^{-8} , 2.02×10^{-8} , and 1.97×10^{-8} $\Omega \text{ m}$ for the surface-cleaned Ag NWs, m-PVP wrapped Ag NWs, and PVP-wrapped Ag NWs. $R_{NW/ET}$ is the contact resistances at the Ag NW/electrode interfaces and can be determined from the single Ag NW device without a NW/NW junction. Therefore, the resistance at the NW/NW junction $R_{NW/NW}$ can be determined, which is $R_{NW/NW} = R_2 - (R_{NW2,1} + R_{NW2,2}) - 2R_{NW/ET}$.

Table S2. Overall resistances and its various components for electron-only devices constructed from surface-cleaned, m-PVP wrapped, and PVP-wrapped Ag NW films with an identical transmittance (85% @550 nm).

Ag NW film	$R_{tot} / \Omega \cdot \text{cm}^{-2}$	$R_{bot} / \Omega \cdot \text{cm}^{-2}$	$R_{top} + R_{t-s} + R_{C60} / \Omega \cdot \text{cm}^{-2}$	$R_{s-b} / \Omega \cdot \text{cm}^{-2}$
Surface-cleaned	297	187	Constant	$110 - (R_{top} + R_{t-s} + R_{C60})$
m-PVP-wrapped	350	217	Constant	$133 - (R_{top} + R_{t-s} + R_{C60})$
PVP-wrapped	3032	2125	Constant	$907 - (R_{top} + R_{t-s} + R_{C60})$

The overall resistance R_{tot} of a device is the sum of each resistance in the circuit (i.e., $R_{tot} = R_{top} + R_{t-s} + R_{C60} + R_{s-b} + R_{bot}$). Here, R_{top} , R_{t-s} , R_{C60} , R_{s-b} , and R_{bot} represent the resistance of the top Ag electrode, the contact resistance at the top Ag electrode/C₆₀ layer junction, the resistance of the C₆₀ layer, the contact resistance at the bottom electrode/C₆₀ layer junction, and the resistance of the Ag NW film, respectively.

Table S3. Comparison of the length (L), diameter (D), and yield (Y) of the Ag NWs synthesized under different conditions using the polyol reduction method and comparison of the sheet resistance (transmittance) of thin transparent films made from these Ag NWs.

Synthesis condition	L / μm	D /nm	Y /%	R_s ($T\%$ ^a) / Ω sq ⁻¹	Ref.
mixed PVP hydrogel as capping ligands	78	64	> 90 (Ag NPs < 3)	32 (88.5)	This work
freshly prepared AgCl as nucleation sites; sealed reaction vessel	10	50	minimal byproducts	n.a.	6
ascorbic acid as auxiliary	270	200	90	322 (92.6)	7
cocamidopropyl betaine and PVP as co-capping ligands	120	130	90	200 (88.7)	8
tetrabutyl ammonium dibromochloride as auxiliary	35	16	n.a.	111 (90.6)	9
prevention of the oxidative etching by CrCl ₃ water as auxiliary	> 75	80	> 90	n.a.	10
	73	45	n.a.	8.1 (81.9)	11
PVP with different molecular weight and concentration as capping ligands	80	78	n.a.	11.4 (81.6)	12
benzyl alcohol as reducing solvent; N-vinylpyrrolidone/N,N-diethylaminoethyl metacrylate copolymer as capping ligands	13	43	n.a.	49.1 (98.6)	13
Cl ⁻ and Br ⁻ as co-additives	84	30-40	> 85	48 (95)	14
mixed polyols (diethylene glycol, triethylene glycol and glycerol) as reducing solvent	66	64	n.a.	4.6 (89.8)	15
limitation of secondary seeding by regulating reaction temperature	34	21	< 50 (Ag NPs < 5)	59 (91.7)	16
NaBr and AgCl as conucleant	11	30	90	12.2 (83.3)	17
PVP and FeCl ₃ as co-capping ligands; hydrothermal synthesis	220	55	92.1	155 (97.7)	18
benzoin as auxiliary; hydrothermal synthesis	40	13	n.a.	28 (95.0)	19

n.a., not available data. The superscript of a in the parenthesis represents the transparency of the thin Ag NW film at 550 nm.

References

1. S. C. Yan, Z. S. Li and Z. G. Zou, *Langmuir*, 2009, **25**, 10397-10401.
2. K. E. Korte, S. E. Skrabalak and Y. N. Xia, *J. Mater. Chem. A*, 2008, **18**, 437-441.
3. W. M. Schuette and W. E. Buhro, *ACS Nano*, 2013, **7**, 3844-3853.
4. Y. Ge, X. Duan, M. Zhang, L. Mei, J. Hu, W. Hu and X. Duan, *J. Am. Chem. Soc.*, 2018, **140**, 193-199.
5. A. Bid, A. Bora and A. K. Raychaudhuri, *Phys. Rev. B*, 2006, **74**, 035426.
6. M. Parente, M. van Helvert, R. F. Hamans, R. Verbroekken, R. Sinha, A. Bieberle-Hutter and A. Baldi, *Nano Lett.*, 2020, 5759-5764.
7. Y. Li, Y. Li, Z. Fan, H. Yang, X. Yuan and C. Wang, *ACS Omega*, 2020, **5**, 18458-18464.
8. Y. X. Li, Y. Li, Z. Y. Fan, H. W. Yang, X. M. Yuan and C. Wang, *Rsc Adv.*, 2020, **10**, 21369-21374.
9. X. Yuan, H. Yang, Y. Li, Y. Li, Y. Chao, J. Chen and L. Chen, *Langmuir*, 2019, **35**, 11829-11835.
10. B. Zhang, R. Dang, Q. Cao, P. Zhao, K. Chen and H. Meng, *J. Nanomater.*, 2019, **2019**, 1-8.
11. W. Zhao, S.-S. Wang, H.-T. Cao, L.-H. Xie, C.-S. Hong, L.-Z. Jin, M.-N. Yu, H. Zhang, Z.-Y. Zhang, L.-H. Huang and W. Huang, *Rsc Adv.*, 2019, **9**, 1933-1938.
12. H. Yang, T. Chen, H. Wang, S. Bai and X. Guo, *Mater. Res. Bull.*, 2018, **102**, 79-85.
13. S. Sugiyama, S. Yokoyama, J. L. Cuya Huaman, S. Ida, T. Matsumoto, D. Kodama, K. Sato, H. Miyamura, Y. Hirokawa and J. Balachandran, *J. Colloid Interface Sci.*, 2018, **527**, 315-327.
14. Y. Rui, W. Zhao, D. Zhu, H. Wang, G. Song, M. T. Swihart, N. Wan, D. Gu, X. Tang, Y. Yang and T. Zhang, *Nanomaterials*, 2018, **8**, 161.
15. T. Chen, H. Wang, H. Yang, S. Bai and X. Guo, *Materials Research Express*, 2018, **5**, 066426.
16. D. Jia, Y. Zhao, W. Wei, C. Chen, G. Lei, M. Wan, J. Tao, S. Li, S. Ji and C. Ye, *Crystengcomm*, 2017, **19**, 148-153.
17. Y. Liu, Y. Chen, R. Shi, L. Cao, Z. Wang, T. Sun, J. Lin, J. Liu and W. Huang, *Rsc Adv.*, 2017, **7**, 4891-4895.
18. Y. Zhang, J. Guo, D. Xu, Y. Sun and F. Yan, *ACS Appl. Mater. Interfaces*, 2017, **9**, 25465-25473.
19. Z. Niu, F. Cui, E. Kuttner, C. Xie, H. Chen, Y. Sun, A. Dehestani, K. Schierle-Arndt and P. Yang, *Nano Lett.*, 2018, **18**, 5329-5334.